ELSEVIER

Journal of Power Sources 89 (2000) 132–138

JOURNAL OF POWER SOURCES

www.elsevier.com/locate/jpowsour

Comparison of lithium-polymer cell performance with unity and nonunity transference numbers

Karen E. Thomas [a,b], Steve E. Sloop [b], John B. Kerr [b], John Newman [a,b,*]

[a] *Department of Chemical Engineering, University of California, Berkeley, CA 94720-1462, USA*

[b] *Environmental Energy Technology Division, Lawrence Berkeley National Laboratory University of California, Berkeley, CA 94720, USA*

Received 29 September 1999; accepted 6 December 1999

Abstract

This work compares the performance of lithium batteries with polymer electrolytes with unity (''ionomer'') and nonunity (''polymer electrolyte'') transference numbers. The study is performed with respect to a particular cell chemistry, Li metal | polymer | LiV_6O_{13}-composite electrode, which is currently a top candidate for use in electric vehicles. Cell performance was modeled to determine the best possible performance of cells containing four different electrolytes: ''ideal'' polymer membrane and ionomer with properties defined by USABC goals, and the presently best available polymer electrolyte and ionomer. Positive electrode thickness, porosity, and current density were varied to find the cell geometry with the highest combined energy density and peak power performance for cells with each electrolyte, and concentration and potential profiles are examined to determine the limitations of the electrolytes. The results show that at 40°C, the ''ideal'' polymer electrolyte can provide 104 W h/kg and 99 W_p/kg, the ''ideal'' ionomer can provide 94 W h/kg and 58 W_p/kg, and the currently available electrolytes can provide about one-fifth of these values. Published by Elsevier Science S.A.

Keywords: Lithium-polymer cell; Unity transference numbers; Nonunity transference numbers

1. Introduction

This study analyzes electrochemical performance of polymer electrolytes in lithium-polymer batteries, the trade-offs between unity (''ionomer'') and nonunity (''polymer electrolyte'') transference numbers, and examines the basis for long-term performance goals for polymer electrolytes for use in electric vehicles that have been developed by the United States Advanced Battery Consortium (USABC). The analysis is performed with respect to a particular cell chemistry, Li metal | polymer | LiV_6O_{13}-composite electrode, which is currently a top candidate for use in electric vehicles. Cell performance was modeled to determine the best possible performance of cells containing four different electrolytes: ''ideal'' polymer electrolyte and an ''ideal'' ionomer with properties defined by USABC goals, and the presently ''best-available'' (best of those tested in this laboratory) polymer electrolyte, oxymethylene-linked poly(ethylene glycol) (PEMO) (molecular weight 400) with lithium bis(trifluoromethylsulfonyl) imide (TFSI), and a best available ionomer, a random copolymer of methylpolyethylene glycol acrylate (molecular weight 500) and lithium sulfonated diethylene glycol acrylate (see Table 1). The transport properties of an ionomer are completely described by the ionic conductivity, which was measured using the technique described in Ref. [5]. Transport in a polymer electrolyte involves two additional properties. Appendix A describes the complete transport properties of the polymer electrolytes used in the simulations.

The positive electrode thickness, porosity, and current density were varied to find the combination which yields the highest product of specific energy for a 3-h galvanostatic discharge and peak specific power for 30 s after 80%

* Corresponding author. Tel.: +1-510-642-4063; fax: +1-510-642-4778.

E-mail address: newman@newman.cchem.berkeley.edu (J. Newman).

0378-7753/00/$ - see front matter. Published by Elsevier Science S.A.
PII: S0378-7753(00)00420-1

Table 1
Transport properties (ionic conductivity, cation transference number, and salt diffusion coefficient) of the electrolytes modeled in this study

	Ideal case (USABC goals)	Best currently available
Polymer electrolyte		
κ (S/cm)	10^{-3}	10^{-4}
t_+^0	0.3	0.1
D (m^2/s)	10^{-11}	6×10^{-13}
Ionomer		
κ (S/cm)	10^{-4}	4×10^{-6}

Table 2
Best combined energy–power performance of Li | LiV_6O_{13} cells with four electrolyte materials, with 50 μm-thick separators

	Polymer electrolytes		Ionomers	
	Available	Ideal	Available	Ideal
Specific energy (W h/kg)	24	104	23	94
Peak specific power (W/kg)	20	88	8	58
Current density (mA/cm^2)	0.15	1.0	0.15	0.95
Positive electrode thickness (μm)	20	90	20	90
Porosity	0.3	0.4	0.4	0.35

of the discharge time (at 2.4 h).[1] The model used has been described by Fuller et al. [1]. The mass used to calculate specific energy and peak specific power includes the mass of the current collectors, active material, conductive filler, and electrolyte, but does not include packaging. The model was run for values of current density ranging from 0.05 to 1.7 mA/cm^2, positive electrode thickness ranging from 10 to 160 μm, and electrolyte volume fraction in the positive electrode ranging from 0.15 to 0.5. For a given application, the required total current will be determined by the load. The current density required for this load, then, is the total current divided by the cell area. Thus, optimizing the current density allows one to calculate the cell area required for a given load. All other parameters used in the model are shown in Appendix B.

2. Results and discussion

Table 2 shows the results of the simulations for an operating temperature of 40°C. One should note that the maximum peak specific power and specific energy listed are those that give the highest combination of energy and power: cells can be designed to increase one at the expense of the other, within the capabilities of the cell chemistry, as needed by a particular application. The ''percent derating'' can be defined as the ratio of the maximum specific energy when the cell is optimized for specific energy to that when the cell is optimized for specific energy and peak specific power combined. For these cells, the derating is approximately 50%.

The polymer electrolyte cells can provide greater specific power than the ionomers because of their higher ionic conductivity. Performance of the ionomers is limited by the ohmic resistance, while the polymer electrolytes are limited by the formation of concentration gradients that lead to salt depletion at the cathode and risk of precipitation at the anode. The ideal electrolytes can be used in thicker cells with more active material per unit area because transport to the active material is not hindered as much as in the best-available electrolytes.

One can gain much insight into the cell performance by examining the state of the cell at the end of the 3-h discharge. For the ionomer, the electrolyte concentration is constant. This restriction has two major effects. First, the reaction-rate distribution in the positive electrode is nearly uniform, varying only due to ohmic drop in the electrolyte. Therefore, the active material (Fig. 1) is filled nearly uniformly across the electrode. Second, there is no concentration overpotential. As a result, the cell with the highest specific energy will be one that has just enough active material to supply the load for the design time of 3 h, after which the cell is completely discharged and the cell voltage will fall abruptly. The currently available ionomer has high ohmic resistance (Fig. 2), and therefore less of the

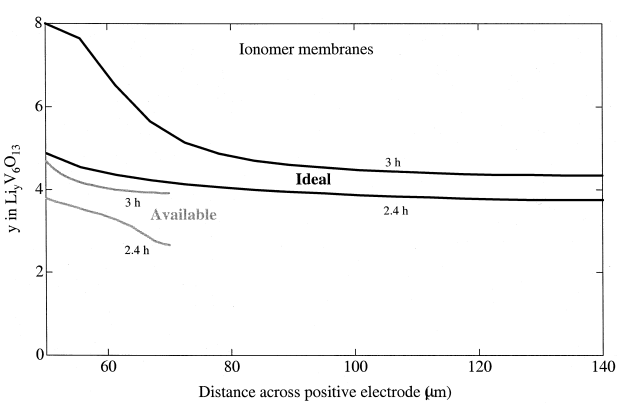

Fig. 1. Active material utilization (expressed as y in $Li_yV_6O_{13}$, where y can range from 0 to 8) across the positive electrode for the best-available and ideal ionomers, with 50 μm separator thickness, after 2.4 and 3 h of discharge at the optimum current density listed in Table 2. The active material reacts nearly uniformly due to the constant electrolyte concentration. A higher fraction of the active material can be utilized with the ideal electrolyte before the cutoff potential is reached because of the lower ohmic losses.

[1] Optimizing the product of specific energy and peak specific power yields a result very close to that obtained when the cell is optimized by finding the largest point which lies on a line whose slope is the ratio of the maximum specific energy to maximum peak specific power, when the cell is optimized for each performance criterion separately, as described in Ref. [2].

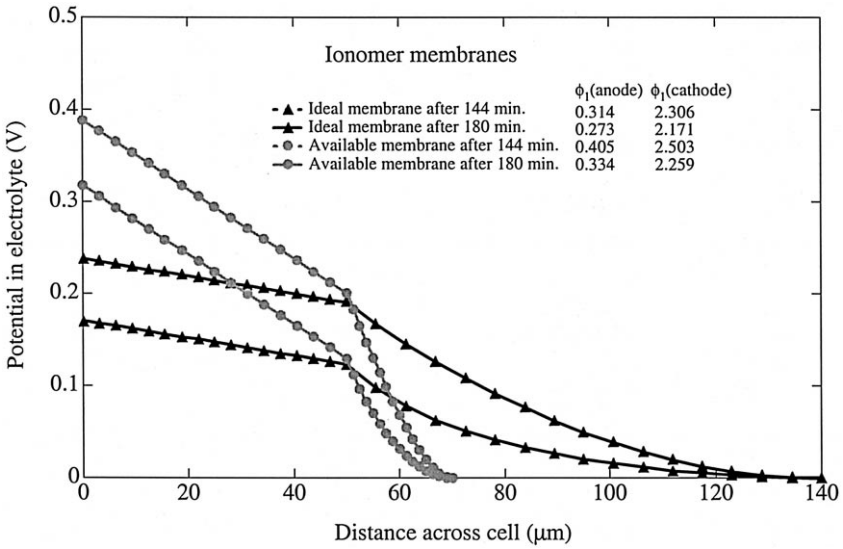

Fig. 2. Electrolyte-phase potential in the best-available and ideal ionomers, after 2.4 and 3 h of discharge at the optimum current density listed in Table 2, and potential at the current collectors, demonstrating the ohmic resistance in the electrolytes.

active material is utilized before the cutoff voltage is reached. Thinner electrodes minimize this ohmic loss.

The performance of the polymer electrolytes is dominated by the concentration profiles (Fig. 3). If the concentration in the cathode is driven to zero, the cell voltage quickly drops. The cell dimensions and current density for any given application must be designed to maintain the salt concentration in the cathode and to prevent salt precipitation at the anode. Concentration gradients in the PEMO–TFSI are exacerbated by the low transference number (see Fig. 6). Therefore, only low current densities can be used in these cells, and most of the active material is not utilized (Fig. 4). In contrast, over 75% of the capacity of the cell with the ideal polymer electrolyte can be used. Fig. 5 shows that the PEMO–TFSI cell has a potential above the cutoff potential at the end of discharge. If one were to design a cell to maximize energy density for a 3-h discharge, the cell would just reach the cutoff potential at the end of 3 h. However, in this study, we have optimized the cells for the highest product of specific energy and specific power. Higher current densities cause larger concentration gradients that greatly inhibit the cell's power pulse performance. In order to maintain a reserve for a power pulse, lower current densities must be used.

USABC goals specify a current density of 1 mA/cm^2 for a design discharge time of 3 h. This current density does provide the maximum combination of specific energy and peak specific power for the ideal electrolytes. Higher current densities would provide higher specific energy at the cost of peak power performance, and conversely lower current densities would give higher peak specific power and lower utilization of the active material. The best currently available electrolyte materials cannot supply such high current densities. The ohmic drop across the low-conductivity ion exchange membrane would drop the voltage

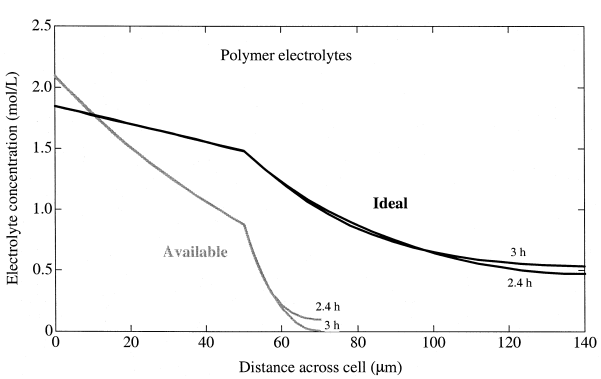

Fig. 3. Electrolyte concentration profile across the separator and positive electrode in the best-available and ideal polymer electrolytes after 2.4 and 3 h of discharge at the optimum current density listed in Table 2.

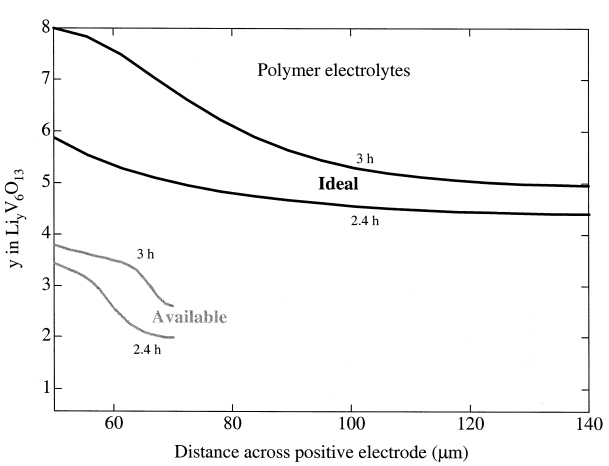

Fig. 4. Active material utilization across the positive electrode for the best-available and ideal polymer electrolytes after 2.4 and 3 h of discharge at the optimum current density listed in Table 2. Because of the large concentration gradients shown in Fig. 3, the reaction rate is highly nonuniform and much of the electrode is not utilized.

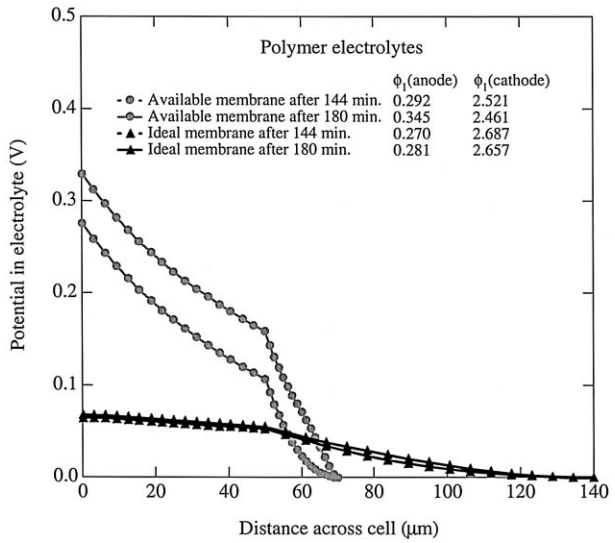

Fig. 5. Electrolyte-phase potential in the 50 μm best-available and ideal polymer electrolytes, after 2.4 and 3 h of discharge at the optimum current density listed in Table 2, and potential at the current collectors.

below tolerable limits for electronic needs. Concentration gradients in the polymer electrolyte would cause a risk of salt precipitation and a high concentration overpotential.

The conductivity at 40°C of PEMO–TFSI at its maximum is the same as that of the ideal ionomer. However, the performance is clearly worse, due to the effects of concentration gradients. In addition, while the conductivity of the ideal ionomer is an order of magnitude lower than that of the ideal polymer electrolyte, its specific energy performance is only 10% lower. From these observations, we conclude that the most significant improvements in polymer electrolytes would be obtained from an increase in the transference number.

Remarkably, at 85°C, the properties of the electrolytes investigated in this work are very close to the USABC goals: t_+^0 is slightly higher (0.5 instead of 0.3), D slightly lower (5×10^{-12} instead of 1×10^{-11} m^2/s, and the conductivity at its maximum is the same value (1×10^{-3} S/cm). Therefore, the performance of the polymer electrolyte at 85°C will be similar to the performance of the ideal polymer electrolyte. The question then arises as to whether it is better to focus on designing an application and cell that can operate with presently available polymer electrolytes and at 85°C, or to focus on synthesizing better polymer electrolytes that can meet the USABC goals at room temperature.

Table 3
Best combined energy–power performance of $Li|LiV_6O_{13}$ cells with available polymer electrolyte and ionomer electrolyte materials, with 10 μm-thick separators

	Available polymer electrolyte	Available ionomer
Specific energy (W h/kg)	37	41
Peak specific power (W/kg)	23	20
Current density (mA/cm^2)	0.20	0.25
Positive electrode thickness (μm)	20	30
Porosity	0.4	0.4

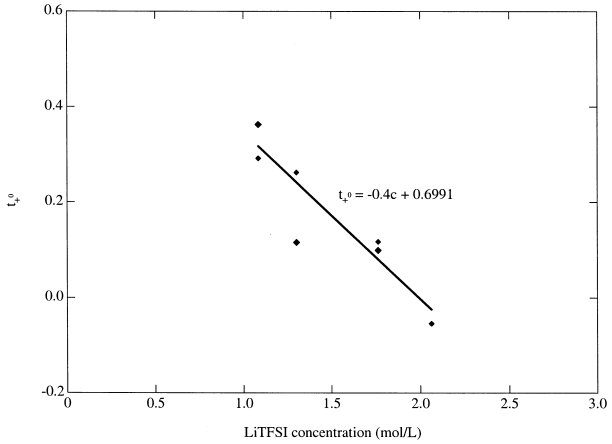

Fig. 6. Transference number of LiTFSI in PEMO at 40°C.

For this study, 50 μm was selected as the separator thickness, in order to maintain a safety margin to ensure separation of the electrodes. Future manufacturing methods may allow thinner separators to be used. To investigate the performance enhancements possible from simply making the separator thinner, cells were optimized for the best currently available polymer electrolyte and ionomer with a separator thickness of 10 μm. Results are shown in Table 3. For separator of one-fifth the thickness, we see that the specific energy almost doubles. The ionomer is able to deliver over twice as much power because of the decreased ohmic drop across the separator (note, however, that the power does not increase by five because much of the resistance is in the porous positive electrode). The peak-power output of the polymer electrolyte does not change significantly because this configuration favored specific energy over peak specific power. We see that while thinner separators do result in improved energy density, the increase is not simply proportional to the decrease in thickness, and greater performance improvements would result from improved transport properties.

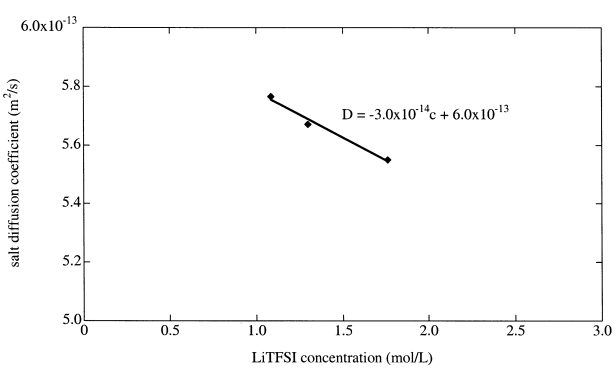

Fig. 7. Salt diffusion coefficient of LiTFSI in PEMO at 40°C.

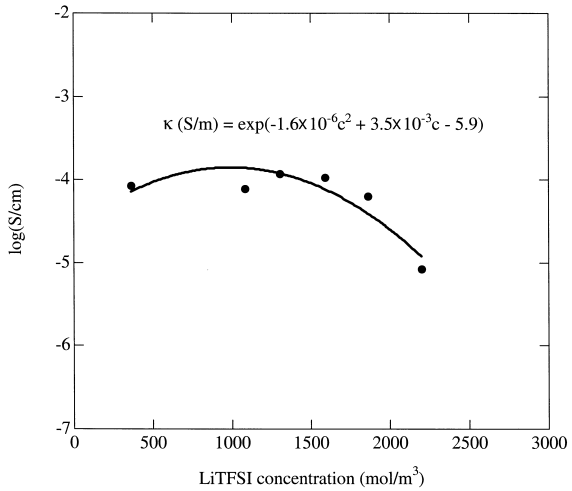

Fig. 8. Log(ionic conductivity) of LiTFSI in PEMO at 40°C.

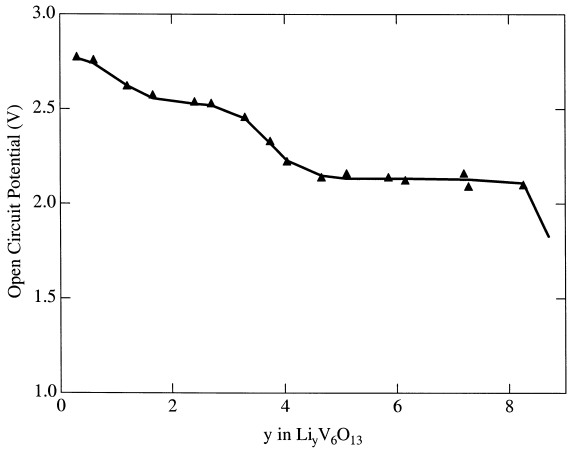

Fig. 10. Open-circuit potential for $Li_yV_6O_{13}$, from Ref. [3].

We note that positive electrode chemistries with higher potentials may be selected for use in lithium-polymer cells. The chemistry selected for this study is that described by West et al. [3] The shape of the open-circuit potential profile (i.e., the shape of sloped and plateau regions) has a significant effect on cell performance, particularly in the polymer electrolytes, due to the effect on the reaction rate distribution across the positive electrode. Therefore, a separate study would be necessary to assess accurately the performance of chemistries with differently shaped open-circuit potential profiles. The effect of merely increasing the open-circuit potential without changing its shape on the specific energy of a cell with a given geometry is linear; i.e., the change in specific energy that would result from using a positive-electrode chemistry with an open-circuit potential 1 V higher than that used in this study would be (1 V) × (current density) × (discharge time)/(cell mass per unit area), or about 9 W h/kg for the best available polymer electrolyte examined here. The effect on peak specific power is more complex and must be determined by separate simulations; for PEMO–TFSI, the increase in peak specific power due to an increase in cell potential of 1 V is approximately 15 W/kg. Note that the above discussion assumes a fixed cell geometry and fixed difference between the initial potential and cutoff potential.

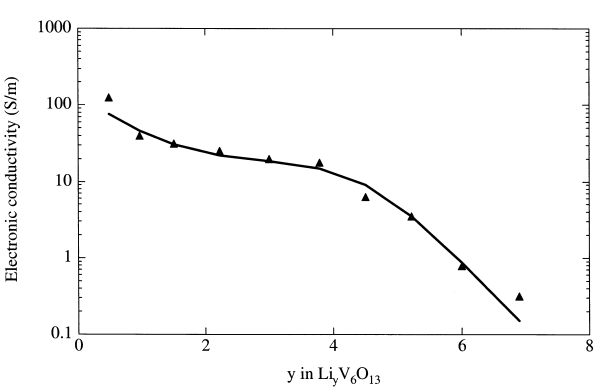

Fig. 9. Electronic conductivity in S/m as function of state of charge, from Ref. [3] corrected for porosity.

3. Conclusion

In this analysis, we have shown that cells operated at 40°C, using the best polymer electrolyte and ionomer synthesized to date in our laboratories, would have approximately one-fifth the specific energy and peak specific power of cells using electrolytes that met USABC goals. The optimum geometry of porous electrodes depends strongly on what one is optimizing for (i.e., energy or power) and the transport properties of the electrolyte. Rather than specifying a current density, one should optimize for the separator area that gives the best overall cell performance. The polymer electrolytes have severe transport limitations. Research into polymer electrolytes should focus on increasing the diffusion coefficient and transference number, not just the conductivity.

The direction of future research efforts should be guided by the needs of the intended applications. Further simulations are necessary to determine whether the available electrolytes could fulfill the energy demands of current applications such as laptop computers or electric vehicles. There is a tradeoff between designing the application and cell to operate at higher temperatures versus trying to synthesize polymers with better transport properties.

Acknowledgements

This material is based upon work supported under a National Science Foundation Graduate Fellowship. This work was supported by the Assistant Secretary for Energy Efficiency and Renewable Energy, Office of Transportation Technologies, Electric and Hybrid Propulsion Divi-

sion of the US Department of Energy under Contract #DE-AC03-76F00098.

Appendix A. Transport properties of polymer electrolytes used in the simulations

The ideal polymer electrolyte was assumed to have transport properties which are independent of concentration. The values used were an ionic conductivity of 0.1 S/m and transference number of 0.3, from USABC goals; a salt diffusion coefficient of 1×10^{-11} m^2/s; and an assumed thermodynamic factor of 1.0.

Properties of PEMO–TFSI were measured at 40°C, using the methods outlined in Refs. [4,5]. An average value of the thermodynamic factor, which is defined as $1 + d(\ln f)/d(\ln c)$, where f is the mean ionic activity coefficient, of 4.3 was used. Least-squares fits to the concentration dependence of the transference number, salt diffusion coefficient, and ionic conductivity are shown in Figs. 6, 7 and 8, respectively.

Appendix B. Parameter values for simulation of Li metal | separator | LiV_6O_{13}

Parameter	Value	Explanation/reference
Li foil thickness		Capacity of negative = 2.5 times capacity of positive electrode
Separator thickness	50 μm	Minimize thickness while preventing short-circuiting
Current collector thicknesses	25 μm	Standard size (1 mil) for Al and Cu foil
Temperature	313 K	Just above room temperature
Initial salt concentration	1300 mol/m^3	Conductivity maximum for polymer electrolytes
Initial y in $Li_yV_6O_{13}$	0.3	Fully charged [3]
Cutoff potential	1.9 V	Prevent lattice degradation, protect electronics [3,6]
Solid diffusion coefficient in positive material	1×10^{-13} m^2/s	[3,6]
Positive material particle radius	10 μm	Estimate to balance power performance with degradation reactions
Volume fraction of carbon in cathode	0.2	See note 1
Electronic conductivity of composite positive electrode	11.45 S/m	See note 1
Exchange current density at negative electrode	3.1 mA/cm^2	[7]. Reference concentration is 1 M
Exchange current density at positive electrode	0.4 mA/cm^2	[3]. Reference concentration is 1 M and y of 1.2
Film resistance at negative electrode	0.01 Ω m^2	Based on Ref. [8]
Coulombic capacity of negative electrode	3862.5 mA h/g	
Coulombic capacity of positive electrode	417.4 mA h/g	Based on y in $Li_yV_6O_{13}$ ranging from 0 to 8 [3]
Density of negative active material	534 kg/m^3	[9]
Density of positive active material	3900 kg/m^3	Interpolated from Ref. [9]
Density of carbon filler	1800 kg/m^3	[9]
Density of polymer electrolyte	1700 kg/m^3	Measured
Density of copper current collector	8954 kg/m^3	[9]
Density of aluminum current collector	2707 kg/m^3	[9]
Open-circuit potential		See note 2
Transfer coefficient	0.5	[7]

B.1. Note 1

West et al. [3] measured the electrical conductivity of a porous compressed electrode of $Li_yV_6O_{12.864}$ as a function of y. The electrical conductivity ranged from 40 S/m at $y = 0.6$ to 0.4 S/m at $y = 6.6$, with an average of 7 S/m (corrected for a porosity of about 0.6). Fig. 9 shows a fit to the data from Ref. [3], using the equation: $\sigma = 9 + 120e^{(-1.5y)} - 9\tanh(y - 4.5)$.

Using the model of Meredith and Tobias [11] for a concentrated mixture of spheres of carbon filler with a modest particle size distribution in a matrix of vanadium oxide, it is calculated that a 20% volume fraction of carbon yields a minimum effective conductivity of 0.64 S/m and an average conductivity of 11.45 S/m. The value used for the electrical conductivity of carbon was 10^5 S/m [12]. The Bruggeman correction is then used to correct the effective conductivity of the matrix for its porosity.

B.2. Note 2

The open-circuit potential, U, of $Li_yV_6O_{13}$ and related nonstoichiometric vanadium oxides has been reported by Refs. [3,6,10], all of which report very similar profiles (Fig. 10). The equation used in this simulation was obtained by a fit to data from Ref. [3] at 25°C, for y ranging from 0 to 8.25:

$$U = 1.9 + 0.13\tanh(-1.67y + 1.7) + 0.2\tanh(-1.67y + 6.2) + 0.56\tanh(-3.33y + 29.5).$$

References

[1] T.F. Fuller, M. Doyle, J. Newman, J. Electrochem. Soc. 141 (1994) 1.
[2] G.G. Trost, V. Edwards, J.S. Newman, Electrochemical reaction engineering, in: J.J. Carberry, A. Varma (Eds.), Chemical Reaction and Reactor Engineering, Marcel Dekker, New York, 1987.
[3] K. West, B. Zachau-Christiansen, T. Jacobsen, Electrochim. Acta 28 (1983) 1829.
[4] Y. Ma, M. Doyle, T.F. Fuller, M.M. Doeff, L.C. De Jonghe, J. Newman, J. Electrochem. Soc. 142 (1995) 1859.
[5] M.M. Doeff, L. Edman, S.E. Sloop, J. Kerr, L.C. De Jonghe, J. Power Sources (2000) this issue.
[6] K.M. Abraham, J.L. Goldman, M.D. Dempsey, J. Electrochem. Soc. 128 (1981) 2493.
[7] M. Verbrugge, AIChE J. 141 (1995) 1550.
[8] M. Doyle, A.S. Gozdz, C.N. Schmutz, J.M. Tarascon, J. Electrochem. Soc. 143 (1996) 1890.
[9] R.H. Perry (Ed.), Perry's Chemical Engineers' Handbook, 4th edn., McGraw-Hill, New York, 1963.
[10] W.J. Macklin, R.J. Neat, S.S. Sandhu, Electrochim. Acta 37 (1992) 1715.
[11] R.E. Meredith, C.W. Tobias (Eds.), Advances in Electrochemistry and Electrochemical Engineering vol. 2 Interscience Publishers, New York, 1962.
[12] R.E. Bolz, G.L. Tuve (Eds.), CRC Handbook of Tables for Applied Engineering Science, 2nd edn., CRC Press, Cleveland, 1976, p. 180.